ELSEVIER

Journal of Biomechanics 35 (2002) 943–950

JOURNAL OF BIOMECHANICS

www.elsevier.com/locate/jbiomech
www.JBiomech.com

Ligament material behavior is nonlinear, viscoelastic and rate-independent under shear loading

Jeffrey A. Weiss*, John C. Gardiner, Carlos Bonifasi-Lista

Department of Bioengineering, The University of Utah, 50 S Central Campus Drive, Rm #2480, Salt Lake City, UT 84112, USA

Accepted 23 February 2002

Abstract

The material behavior of ligament is determined by its constituents, their organization and their interaction with each other. To elucidate the origins of the multiaxial material behavior of ligaments, we investigated ligament response to shear loading under both quasi-static and rate-dependent loading conditions. Stress relaxation tests demonstrated that the tissue was highly viscoelastic in shear, with peak loads dropping over 40% during 30 min of stress relaxation. The stress relaxation response was unaffected by three decades of change in shear strain rate (1.3, 13 and 130%/s). A novel parameter estimation technique was developed to determine material coefficients that best described the experimental response of each test specimen to shear. The experimentally measured clamp displacements and reaction forces from the simple shear tests were used with a nonlinear optimization strategy based around function evaluations from a finite element program. A transversely isotropic material with an exponential matrix strain energy provided an excellent fit to experimental load–displacement curves. The shear modulus of human MCL showed a significant increase with increasing shear strain ($p<0.001$), reaching a maximum of 1.72 ± 0.4871 MPa. The results obtained from this study suggest that viscoelasticity in shear does not likely result from fluid flow. Gradual loading of transversely oriented microstructural features such as intermolecular collagen crosslinks or collagen-proteoglycan crosslinking may be responsible for the stiffening response under shear loading.

Keywords: Shear; Ligament; Soft tissue mechanics; Anisotropic; Finite element

1. Introduction

The contribution of a ligament to joint stability is determined by geometry, shape of the articulating joint surfaces, location and type of insertions to bone, in situ strains and material properties. The structural response of normal ligament is highly dependent on its material properties, and injury and subsequent healing alter material properties. A quantitative description of changes in ligament material properties following injury, during healing, or in response to specific treatment regimens can be obtained via constitutive models. Appropriate models can also elucidate structure–function relations and quantify the relative importance of different microstructural features such as collagen properties, crosslinking and rate-dependence through solid or fluid phase viscoelasticity. Additionally, constitutive models can be used in conjunction with techniques such as the finite element (FE) method to predict normal and pathologic joint function, examine injury mechanisms, and study surgical repair and reconstruction.

The distribution of stress and strain in knee ligaments is highly inhomogeneous under in vivo loading conditions (Gardiner et al., 2001; Hollis et al., 1991; Hull et al., 1996; Livesay et al., 1995, 1997; Markolf et al., 1993; Pfaeffle et al., 2000; Wang et al., 1973; Warren et al., 1974). Thus a three-dimensional constitutive framework is necessary for accurate stress predictions. Transverse isotropy has been used successfully to describe ligament material symmetry (Hannafin and Arnoczky, 1994; Hirokawa and Tsuruno, 2000; Hurschler et al., 1997; Kohles et al., 1997; Lanir, 1980; Puso and Weiss, 1998; Simbeya et al., 1992; Weiss et al., 1996). The physical interpretation of transversely isotropic symmetry is that of a matrix reinforced with a single fiber family. The material behavior arises from matrix properties, fiber–matrix interactions and fiber–fiber interactions. Thus a

*Corresponding author. Tel.: +1-801-587-7833; fax: +1-801-585-5361.

E-mail address: jeff.weiss@utah.edu (J.A. Weiss).

0021-9290/02/$ - see front matter
PII: S0021-9290(02)00041-6

single uniaxial test is insufficient to characterize the three-dimensional material behavior of ligaments. Together, these observations demonstrate that experimental data on the multiaxial quasi-static and viscoelastic material properties of the tissue are necessary for accurate representation of ligament mechanics.

The resistance of ligament to shear loading controls load transfer between different parts of the tissue. When a transversely isotropic material is subjected to simple shear loading parallel to the fiber direction, the fibers will not strain and the resistance will be governed by the matrix behavior and fiber–fiber interactions (Gardiner and Weiss, 2001). In the case of ligament, this eliminates the normally dominant tensile material behavior of collagen from the tissue response and thus allows information to be obtained regarding the status of microstructural features of the tissue such as collagen crosslinking.

The overall objective of this study was to characterize the material response of ligament to simple shear loading. The medial collateral ligament (MCL) was chosen for study because it is one of the most frequently injured ligaments in the knee (Fetto and Marshall, 1978; Miyasaka et al., 1991), it plays a critical role in valgus and anterior–posterior knee stability and it provides an ideal ligamentous structure for multiaxial materials characterization because of its relative planar geometry. Simple shear deformation causes minimal change in volume (Gardiner and Weiss, 2001), and fluid flow is likely to be responsible for at least part of the rate-dependent behavior of ligaments. Thus it was hypothesized that the viscoelastic response of the human MCL to shear would exhibit minimal rate-dependence. We further hypothesized that the shear modulus along the direction of the collagen fibers would stiffen with increasing shear strain due to gradual recruitment of crosslinks between collagen fibers. To test this hypothesis, a novel and robust method was developed to estimate material parameters for a transversely isotropic hyperelastic constitutive model using experimental data from tests and simulation data from FE analysis.

2. Materials and methods

2.1. Specimen preparation

Five human cadaveric MCLs were tested in shear (55 ± 16 years, 4 males, 1 female). The MCL is a large, relatively thin, broad ligament that can be visualized without dissection of the joint capsule. Rectangular specimens were harvested from the anterior region of the human MCL, just distal to the medial meniscus, using a 10×25 mm hardened steel punch. This location was chosen because it was most uniform in thickness, fiber orientation and color between specimens (Quapp and Weiss, 1998). Specimen dimensions and loading conditions were chosen based on a previous FE parameter study that assessed the sensitivity of the strain field to changes in specimen aspect ratio (Gardiner and Weiss, 2001).

2.2. Material testing

Specimens were mounted in a set of custom clamps on a material testing machine (MTS, Eden Prairie, MN) with the fiber direction oriented vertically and subjected to a finite strain simple shear deformation (Fig. 1). The initial width, height and thickness of each specimen were measured three times with digital calipers, and averages were used in all calculations that required these dimensions. Measurements were taken with the aid of a lighted magnification lens and caliper jaws were closed slowly until no light could be seen passing between the tissue and the caliper jaws. Clamp screws were tightened uniformly. Our previous work demonstrated that clamping prestrain has a negligible effect on the predicted strain distribution in the test specimen (Gardiner and Weiss, 2001). Testing was performed at room temperature and specimens were kept continuously moist with 0.9% normal saline during the entire test sequence. Specimens were allowed to equilibrate in a stress-free configuration for 30 min before the testing sequence. A sawtooth displacement profile was then applied at a shear strain rate of 1.3%/s, with a shear strain amplitude of $\tan(\theta) = 0.4$ for 10 cycles based on the measured width of each specimen (Fig. 2A). This amplitude was chosen based on pilot testing to determine the maximum shear strain that could be consistently applied without damage to the specimen as indicated by a drop in load during application of shear strain. Clamp reaction force (measured with a 10 N load

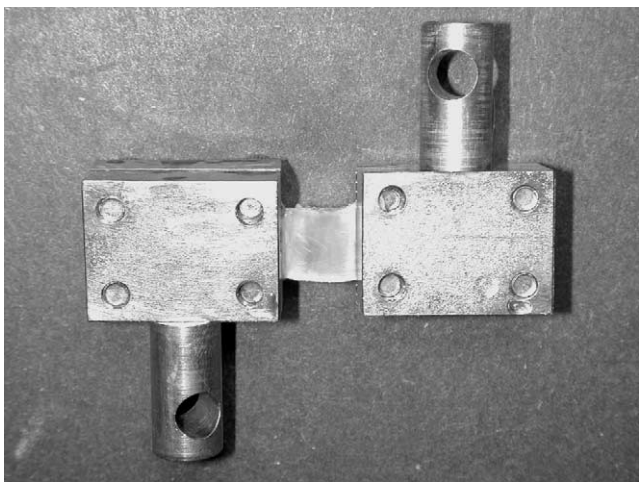

Fig. 1. MCL test sample mounted for simple shear testing in custom clamps.

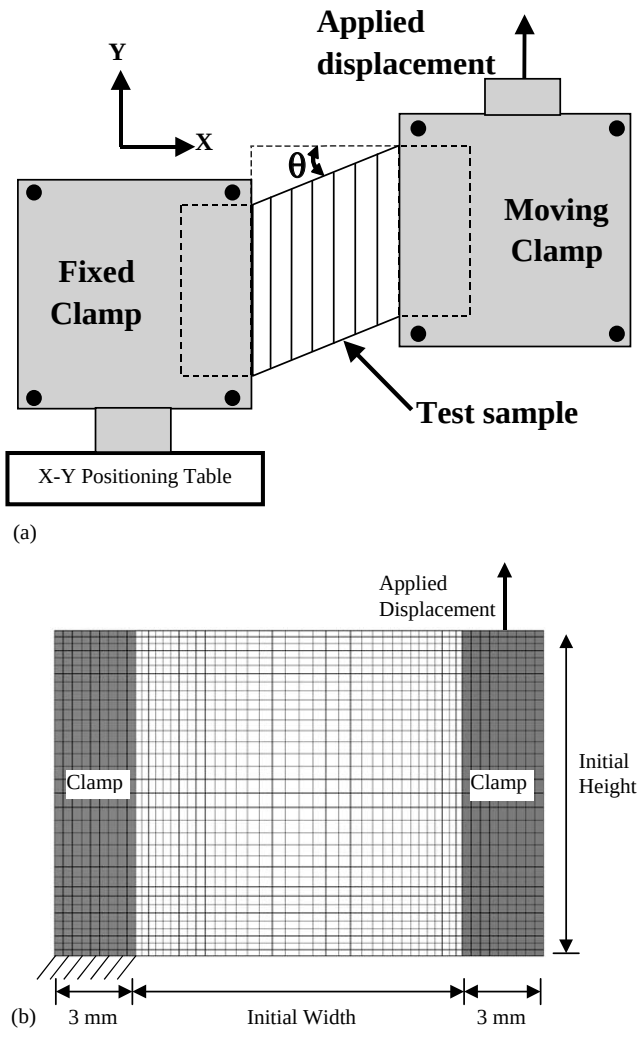

Fig. 2. (A) Schematic of test configuration. One of the clamps was mounted to an X–Y positioning table to facilitate alignment, while the other clamp was attached to a moving crosshead. The test sample was oriented so that the fibers were aligned with the vertical movement axis of the test machine. (B) FE mesh and boundary conditions used in the parameter optimization studies. Three millimeters of the specimen were simulated as clamped. The left clamped section was fixed on the surfaces, while the right clamped section was prescribed displacements corresponding to the experimentally measured crosshead displacement. Test specimen dimensions were assigned using specimen-specific experimental measurements for each simulation.

cell, Transducer Techniques, Temecula, CA) and crosshead displacement were continuously recorded during testing. Global applied shear strain was computed using the specimen initial dimensions and crosshead displacement measurements. The clamp reaction force and global applied shear strain from the loading portion of the 10th cycle were used for the parameter estimation studies described below.

Following cyclic testing and a subsequent 30 min recovery period, consecutive stress relaxation tests were performed at three different strain rates (1.3, 13, and 130 %/s) with a strain amplitude of $\tan(\theta) = 0.4$. For each strain rate, the specimen was allowed to stress-relax for 30 min, followed by a 30-min recovery period. The relaxation time was based on preliminary testing that showed no measurable change in the force after 30 min. During three pilot tests, the stress relaxation test at a strain rate of 1.3%/s was repeated and the response was unaffected by the intervening tests at 13 and 130%/s, demonstrating that damage and preconditioning did not affect the results due to the order of testing. An effective shear stress was defined as the clamp reaction force divided by the sample cross-sectional area. The peak and equilibrium effective shear stresses for the static stress relaxation tests were calculated from the data for each of the three strain rates.

2.3. Constitutive model

For material parameter estimation, the ligament was represented as a fiber-reinforced composite with transversely isotropic material symmetry using a hyperelastic strain energy that uncoupled deviatoric and dilational behavior (Weiss et al., 1996):

$$W = F_1(\tilde{I}_1, \tilde{I}_2) + F_2(\tilde{\lambda}) + U(J) \tag{1}$$

The functions F_1 and F_2 represent the matrix and fiber family strain energies, respectively, and together they compose the entire deviatoric response of the material. $\tilde{I}_1$ and $\tilde{I}_2$ are the deviatoric invariants of the right deformation tensor, and $\tilde{\lambda}$ is the deviatoric local fiber stretch. $U(J)$ governed the dilational response of the material:

$$U(J) = \frac{K}{2}\ln(J)^2, \tag{2}$$

where J is the volume ratio and K represents the effective bulk modulus of the material. An uncoupled deviatoric/dilational constitutive formulation has numerical advantages for simulating nearly incompressible material behavior with the FE method (Weiss et al., 1996), and the formulation is identical to the fully coupled strain energy in the limit of incompressibility or for an isochoric deformation ($J = 1$ for both cases).

The experimental data demonstrated stiffening behavior for the clamp force vs. clamp displacement (Fig. 4). Since there should be minimal stretch along the fiber direction for simple shear, this stiffening behavior must be due to contributions from the matrix response, the fiber–matrix response, or fiber–fiber interactions. It was assumed that this stiffening behavior was due to the matrix strain energy, F_1. After testing several forms for F_1, a form introduced by Veronda and Westmann (Veronda and Westmann, 1970) was adopted:

$$F_1 = C_1[\exp(C_2(\tilde{I}_1 - 3)) - 1] - \frac{C_1 C_2}{2}(\tilde{I}_2 - 3). \tag{3}$$

This strain energy is convex and exhibits physically reasonable behavior under tension, compression and

shear. F_2 was defined as per our previous studies (Gardiner and Weiss, 2001; Quapp and Weiss, 1998):

$$\tilde{\lambda}\frac{\partial F_2}{\partial \lambda} = 0, \quad \tilde{\lambda} < 1,$$

$$\tilde{\lambda}\frac{\partial F_2}{\partial \lambda} = C_3[\exp(C_4(\tilde{\lambda} - 1)) - 1], \quad 1 < \tilde{\lambda} < \lambda^*, \tag{4}$$

$$\tilde{\lambda}\frac{\partial F_2}{\partial \lambda} = C_5\tilde{\lambda} + C_6, \quad \tilde{\lambda} \geqslant \lambda^*.$$

The fiber stress is exponentially stiffening up to a level of fiber stretch λ^*, after which the fiber stress–strain behavior is linear. The values for the fiber family material coefficients, $C_3 - C_5$, were taken from our previous work ($C_3 = 2.45$, $C_4 = 30.6$, $C_5 = 323.7$ (Quapp and Weiss, 1998)), and C_6 followed from the condition that the stress must be at least C_0 continuous at $\lambda = \lambda^*$.

The bulk modulus for each sample was chosen so that the ratio of initial bulk modulus to initial shear modulus was 1000:1. Using the forms for F_1 and F_2 specified above, the Cauchy shear stress T_{12} can be expressed in terms of the shear strain $\kappa = \tan(\theta)$ for a simple shear test as

$$T_{12} = C_1C_2(2\exp(C_2\kappa) - 1)K. \tag{5}$$

Note that the shear modulus is $C_1C_2(2\exp(C_2\kappa))$. When $\kappa = \tan(\theta) = 0$, the shear modulus is C_1C_2, and thus the bulk modulus K was chosen so that:

$$\frac{K}{C_1C_2} = 1000. \tag{6}$$

The true bulk behavior of the tissue was unknown and unavailable in the literature; the chosen ratio provided nearly incompressible material behavior (Simo and Hughes, 1998). It was demonstrated previously that the initial bulk modulus had very little effect on the predicted response of ligament to finite shear because the deformation remained nearly isochoric regardless of the choice of K (Gardiner and Weiss, 2001).

2.4. Parameter estimation technique

To circumvent the difficulty of inhomogeneous deformation during shear loading, a parameter estimation technique was developed and used in conjunction with the FE method to determine the material coefficients that best predicted the experimental response of each test specimen to shear. The loading portion of the 10th cycle of each experiment was simulated using the FE method and material coefficients were iteratively adjusted to match experimentally observed behavior. FE models were constructed for each test specimen using specimen-specific measurements of width, height and thickness. The thickness was assumed to be spatially homogeneous based on pilot work that demonstrated spatial variations in thickness of <0.1 mm. The FE mesh topology was refined via a convergence study to ensure sufficient mesh density. The final mesh consisted of 7072 hexahedral elements. Boundary conditions were applied through the nodes that were in contact with the clamps (Fig. 2B). The tissue extended 3 mm into each clamp and was assumed to be perfectly bonded to the clamp. Experimental loading was simulated by prescribing a translation along the y-axis to nodes contacting the right clamped surfaces to induce a shear of $\tan(\theta) = 0.4$. To simulate experimental conditions, the clamped surfaces were constrained along the x-axis during application of shear strain.

A nonlinear optimization program was written to minimize the sum of squares difference between the experimental force–displacement behavior and the predicted response from the corresponding FE model for each specimen (Fig. 3). Starting values were chosen for material parameters C_1 and C_2 characterizing the matrix, and these were iteratively improved using a sequential quadratic programming method in the NAG Fortran77 Library routine E04UNF (Numerical Algorithms Group, Oxford, England). The NAG routine minimized a smooth objective function subject to a set of constraints on the variables. The objective function $F(x)$ had the form:

$$F(x) = \frac{1}{2}\sum_{i=1}^{m}(y_i - f(x_i))^2. \tag{7}$$

Here, the y_i were the experimentally measured values for clamp reaction force evaluated at m displacement levels

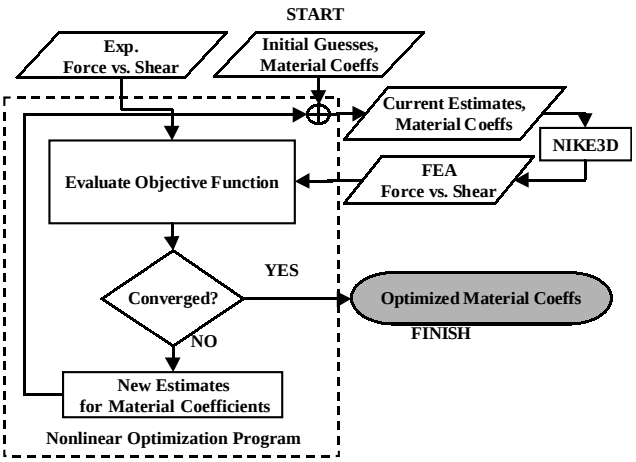

Fig. 3. Diagram of the procedure used for material parameter optimization. The experimentally measured data for movement of the right clamp were used to drive the movement of the simulated FE model on a specimen-specific basis. Using initial guesses for the material parameters C_1 and C_2, the FE model was analyzed to determine the predicted clamp reaction force. This was compared to the experimental reaction force as a function of shear strain level using a nonlinear least squares approach. The material coefficients were iteratively adjusted so that the FE predictions matched the experimental data.

and the $f(x_i)$ were the corresponding predicted values from the nonlinear FE analysis. The NAG subroutine incorporated an augmented Lagrangian merit function and a quasi-Newton approximation to the Hessian (matrix of second partial derivatives). The nonlinear FE program NIKE3D was used to generate the predicted response to finite simple shear (Maker et al., 1990). The entire process was implemented in a wrapper program that repeatedly called the FE program with updated material parameters. This program also performed polynomial interpolation of the resulting force and displacement values from the FE program, allowing the FE program to automatically adjust the stepsize as needed to maintain convergent behavior during the incremental-iterative solution process. The effect of starting values for the material parameters C_1 and C_2 was assessed for one of the five specimens used in the parameter optimization runs. Data for this same specimen were used to assess the effect of the bulk:shear ratio using ratios of 500, 1000, 2000 and 5000 as defined by Eq. (6).

2.5. Statistical analysis

The effect of strain rate on effective shear stress and the ratio of peak/equilibrium effective shear stress were assessed using one-way ANOVAs with repeated measures. Shear modulus was computed as a function of shear strain level for each specimen using Eq. (5) and the effect of strain level on shear modulus was assessed using a one-way ANOVA with repeated measures. Post-hoc Tukey tests were performed between different levels of a factor when significance was found for an ANOVA. Significance was set at $p \leqslant 0.05$ for all statistics.

3. Results

The average dimensions of the test specimens were 10.2 ± 1.1 mm width, 10.2 ± 0.1 mm height and 1.6 ± 0.3 mm thickness. None of the samples showed signs of tissue failure or slippage at the clamps at shear strain levels of up to $\tan(\theta) = 0.4$ for either the cyclic or the stress relaxation tests. Despite the large amount of shear strain, the resulting stresses were <1 MPA. The effective shear stress–strain relationship was highly nonlinear (Fig. 4).

Stress relaxation testing demonstrated a large amount of relaxation regardless of strain rate (Fig. 5). There was no effect of strain rate on the peak stress ($p = 0.98$) or the ratio of the peak/equilibrium stress ($p = 0.445$). For each sample, the load–displacement curve from the loading part of the stress relaxation test was nearly identical for all three strain rates.

The nonlinear optimization program was successful in minimizing the difference between experimental and FE

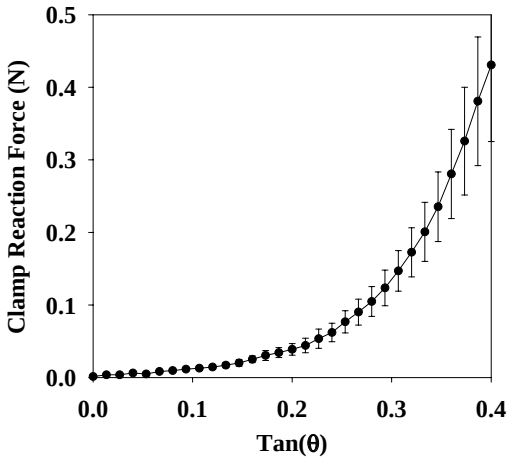

Fig. 4. Experimental clamp reaction force as a function of applied shear strain as measured in terms of clamp displacement. The response stiffened rapidly after a value of $\tan(\theta) = 0.2$ Mean $\pm$ std error.

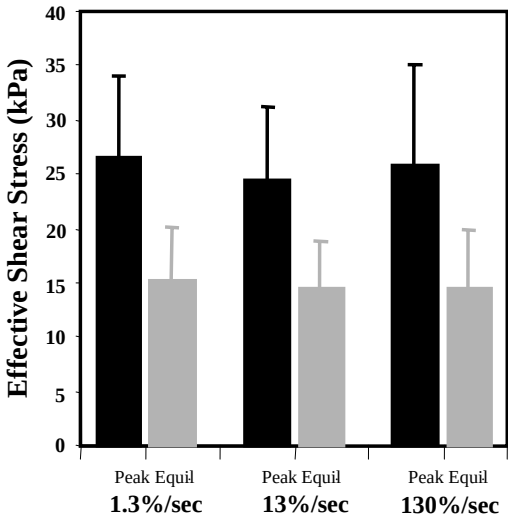

Fig. 5. Effect of strain rate on peak and equilibrium stresses during a stress relaxation test. There was no significant change in the viscoelastic response with increasing shear strain rate. Mean $\pm$ std error.

force–displacement data for all specimens using the default convergence criteria in the NAG routine. The optimization runs took 0.5–5.0 h on four processors of an SGI Origin 2000 (R10000 processor) and each optimization run required 60–200 executions of NIKE3D. The fit of the experimental force–displacement data to that predicted by parameter optimization was excellent in all cases, as demonstrated by R^2 values that were always >0.995 (Table 1, column 5). There was no effect of changes in the starting values for the two material parameters on the resulting best-fit parameters as determined by the nonlinear optimization program.

The magnitude of C_1, which scales the matrix stress response, demonstrated considerable variation between

Table 1
Optimized material coefficients for the matrix behavior of the MCL. The coefficient scaling the stress response C_1 demonstrated significant variation between samples, while the coefficient controlling the rate of stiffening C_2 exhibited a smaller deviation. There was little effect of the assumed bulk/shear ratio on the predicted material coefficients

Sample #	Bulk/shear ratio	C_1 (Pa)	C_2	R^2
1	1000	1059.7	11.08	0.999
2	1000	300.5	9.23	0.997
3	1000	1644.1	9.73	0.998
4	1000	697.7	11.37	0.995
5	1000	460.2	13.86	0.996
Mean $\pm$ std		832.4 $\pm$ 536.2	11.05 $\pm$ 1.81	
3	500	1625.6	9.81	0.999
3	2000	1652.0	9.70	0.998
3	5000	1675.0	9.63	0.998

samples (Table 1, column 3). This reflects the variation in force–displacement curves that were obtained during experiments, as suggested by the error bars in Fig. 2. In contrast, the coefficient C_2 that controls the rate of rise of exponential matrix stresses exhibited much less variation (Table 1, column 4). Thus the general shape of the response curve was consistent between samples. Changes in the bulk:shear ratio resulted in small changes in the material coefficients. A change of one order of magnitude produced a 3% change in the optimal value for C_1 and a 5% change in the optimal value for C_2.

There was a significant increase in shear modulus with increasing levels of shear strain ($p<0.001$). In particular, Tukey tests demonstrated that the shear moduli at $\kappa = 0.1$ (45.1 ± 9.8 kPa), $\kappa = 0.2$ (157.6 ± 33.2 kPa) and $\kappa = 0.3$ (516.9 ± 120.9 kPa) were all significantly different than the shear modulus at $\kappa = 0.4$ (1696.2 ± 487.1 kPa). There was no significant difference for comparisons at shear strain levels of 0.1 vs. 0.2, 0.2 vs. 0.3 and 0.1 vs. 0.3.

4. Discussion

This study characterized the elastic and viscoelastic response of the human MCL to simple shear loading along the fiber direction to gain insight into structure–function relationships in ligamentous tissue. A combined experimental and computational procedure yielded quantitative description of the material parameters. The shear stiffness of human MCL increased dramatically with increasing shear strain, and the shape of the curve and its magnitude were independent of strain rate. Stress relaxation testing at three different strain rates demonstrated that there was no significant effect of strain rate on peak or equilibrium loading values, yet a 40% reduction in peak load occurred during relaxation at all strain rates tested.

These was a significant increase in shear modulus with applied shear strain. This is in contrast to data from transverse tensile testing of human MCL (Quapp and Weiss, 1998), which demonstrated that the transverse tensile stress–strain behavior is linear. This strongly suggests that shearing causes microstructural change, reorganization or gradual recruitment of a microstructural feature. An increase in shear modulus with applied shear strain could be produced by fiber–fiber bonds with linear stress–strain behavior under tension, and this model would still provide a consistent description of the transverse tensile behavior. Perhaps the most likely candidate is intermolecular crosslinking. Both hydroxyproline crosslink density (Frank et al., 1995; Woo et al., 1997) and hydroxypyridinium crosslink density (Ng et al., 1996; Salehpour et al., 1995) are positively correlated with modulus in ligaments and tendons. Molecular crosslinking between collagen and proteoglycans could also be the cause of the stiffening behavior. It has been demonstrated that the resistance of cartilage to shear is highly dependent on the chemical status of proteoglycans, and shear modulus is greatly reduced when proteoglycans are degraded (Zhu et al., 1993). The exact mechanism of stiffening in shear could be clarified using selective chemical degradation to target specific crosslink types.

A large amount of relaxation was observed during the shear stress relaxation experiments. However, there was little change in peak effective stress or the ratio of peak/equilibrium effective stress with strain rate. This suggests that the damping and stiffness associated with viscoelasticity under shear are relatively constant over a range of strain rates. Constant damping over a range of frequencies has been observed in many soft tissues under tensile loading, but most tissues exhibit at least a moderate stiffening with increasing strain rate. When ligament is subjected to tensile testing at different strain rates, it exhibits some strain-rate dependence and less drop in stress during relaxation as compared to the shear loading (Danto and Woo, 1993). Thus, the mechanism governing viscoelasticity under shear loading may be fundamentally different than that governing viscoelasticity under tensile loading. Since the finite simple shear test configuration causes minimal volumetric change in the tissue, ligament viscoelastic behavior under shear may depend more on solid phase viscoelasticity rather than fluid flow. There is some evidence that crosslink density influences the viscoelasticity of healing ligament (Thornton et al., 2000), and thus crosslinking may govern both the quasi-static and viscoelastic response of ligament to shear.

There appears to be only one other report in the literature that examined the experimental shear response of ligament (Wilson et al., 1997). Incising the rabbit MCL at two positions along the length of the ligament on opposite sides and then testing the ligament in

tension resulted in a combined state of tension and shear. The test condition yielded a highly inhomogeneous deformation, and also included stretching along the collagen fiber direction. The magnitude of the resulting forces under shear in the present study is much smaller than that of this previous study. This is likely due to the fact that the tensile resistance of collagen dominated the measured stresses in the previous study.

The parameter estimation technique provided a robust means to fit the experimental load–displacement behavior to specimen-specific FE models. In this case, an exponential function was chosen for the matrix and material coefficients C_1 and C_2 were determined using the iterative technique. It is worth noting that as values of C_1 became small during the parameter estimation procedure, numerical difficulties were sometimes encountered in the incremental-iterative process used to obtain the FE solution. These difficulties were traced to the relative degree of anisotropy in the material. As the ratio of effective longitudinal/transverse "modulus" became very large, numerical ill conditioning was observed in the spatial elasticity tensor corresponding to the hyperelastic material model. This problem was then passed to the global stiffness matrix during the FE assembly process, resulting in a poorly conditioned global stiffness matrix, an inaccurate answer for the inverted stiffness, and finally a poor estimate for the next increment in displacements. This resulted in extra iterations to obtain a converged solution. It is unlikely that this difficulty is specific to the particular constitutive model used in this study, as this problem is often encountered in nonlinear FE analyses involving highly anisotropic materials.

There was a small effect of bulk modulus on the optimal material coefficients as determined by a parameter study for one of the specimens (Table 1). Our previous analysis of the simple shear configuration with a neo-Hookean matrix strain energy demonstrated minimal effect of the bulk modulus on the predicted strain distribution (Gardiner and Weiss, 2001). Since the present study utilized a very different matrix strain energy, the particular form of the matrix strain energy may not have a large effect on the sensitivity to bulk behavior under shear loading. This result is consistent with the fact that the simple shear test configuration produces a nearly isochoric deformation.

An exponential matrix strain energy provided an excellent description of the observed stiffening behavior under shear loading. However, other matrix strain energy functions could describe the data equally well. The choice of the form in Eq. (3) was made based on its previous use in the literature (Veronda and Westmann, 1970) as well as its convexity, ensuring numerical stability for the FE analyses. In the context of transversely isotropic material symmetry, there are other ways to achieve a stiffening response in shear. Criscione et al. (2001) reported on the development of a new, physically motivated set of invariants for describing transversely isotropic hyperelastic materials, and one of the invariants is directly proportional to shear strain. Using this approach, one could formulate a constitutive model that exhibited stiffening behavior in shear while not affecting the transverse tensile behavior.

The parameter optimization approach developed in conjunction with this study has several limitations. The form of the strain energy function was specified a priori and additional forms were not examined. Further, cross-validation of the predicted material coefficients was not made with independent material test data. The experimental test configuration that was simulated requires a planar structure with relatively uniform thickness and fiber orientation. Such a test specimen would be impossible to obtain for many ligaments. Finally, the parameter estimation approach is computationally expensive. The above limitations are offset by the ease of obtaining the necessary experimental data for the simple shear test, since strain measurement is not necessary to use the optimization strategy.

The results of this study indicate that the material response of human MCL to shear is highly viscoelastic, rate-insensitive and is likely governed by microstructural change or crosslink recruitment. These data can be used in combination with other multiaxial material data to formulate structurally based constitutive models that have separate mechanisms for shear and bulk viscoelasticity, providing improved representations of ligament material properties for experimental studies of healing and numerical simulation of joint mechanics. The ability to utilize experiments that produce inhomogeneous strain fields should provide more robust estimates for material coefficients via parameter estimation.

Acknowledgements

Support from NIH Grant #AR47369 and a Whitaker Foundation Transition Grant is gratefully acknowledged. An allocation of computer time was provided by the Center for High Performance Computing (CHPC) at the University of Utah. CHPC's SGI Origin 2000 system is funded in part by the SGI Supercomputing Visualization Center Grant.

References

Criscione, J.C., Douglas, A.S., Hunter, W.C., 2001. Physically based strain invariant set for materials exhibiting transversely isotropic behavior. Journal of the Mechanics and Physics of Solids 49, 871–897.

Danto, M.I., Woo, S.L.-Y., 1993. The mechanical properties of skeletally mature rabbit anterior cruciate ligament and patellar

tendon over a range of strain rates. Journal of Orthopaedic Research 11, 58–67.

Fetto, J.F., Marshall, J.L., 1978. Medial collateral ligament injuries of the knee: a rationale for treatment. Clinical Orthopaedics and Related Research 132, 206–218.

Frank, C., McDonald, D., Wilson, J., Eyre, D., Shrive, N., 1995. Rabbit medial collateral ligament scar weakness is associated with decreased collagen pyridinoline crosslink density. Journal of Orthopaedic Research 13, 157–165.

Gardiner, J.C., Weiss, J.A., 2001. Simple shear testing of parallel-fibered planar soft tissues. ASME Journal of Biomechanical Engineering 123, 170–175.

Gardiner, J.C., Weiss, J.A., Rosenberg, T.D., 2001. Strain in the human medial collateral ligament during valgus loading of the knee. Clinical Orthopaedics and Related Research 391, 266–274.

Hannafin, J.A., Arnoczky, S.P., 1994. Effect of cyclic and static tensile loading on water content and solute diffusion in canine flexor tendons: an in vitro study. Journal of Orthopaedic Research 12, 350–356.

Hirokawa, S., Tsuruno, R., 2000. Three-dimensional deformation and stress distribution in an analytical/computational model of the anterior cruciate ligament. Journal of Biomechanics 33, 1069–1077.

Hollis, J.M., Takai, S., Adams, D.J., Horibe, S., Woo, S.L.-Y., 1991. The effects of knee motion and external loading on the length of the anterior cruciate ligament (ACL): a kinematic study. ASME Journal of Biomechanical Engineering 113, 208–214.

Hull, M.L., Berns, G.S., Varma, H., Patterson, H.A., 1996. Strain in the medial collateral ligament of the human knee under single and combined loads. Journal of Biomechanics 29, 199–206.

Hurschler, C., Loit-Ramage, B., Vanderby, R., 1997. A structurally based stress–stretch relationship for tendon and ligament. ASME Journal of Biomechanical Engineering 119, 392–399.

Kohles, S.S., Thielke, R.J., Vanderby, R., 1997. Finite elasticity formulations for evaluation of ligamentous tissue. Biomedical Materials and Engineering 7, 387–390.

Lanir, Y., 1980. A microstructure model for the rheology of mammalian tendon. ASME Journal of Biomechanical Engineering 102, 332–339.

Livesay, G.A., Fujie, H., Kashiwaguchi, S., Morrow, D.A., Fu, F.H., Woo, S.L.-Y., 1995. Determination of the in situ forces and force distribution within the human anterior cruciate ligament. Annals of Biomedical Engineering 23, 467–474.

Livesay, G.A., Rudy, T.W., Woo, S.L.-Y., Runco, T.J., Sakane, M., et al., 1997. Evaluation of the effect of joint constraints on the in situ force distribution in the anterior cruciate ligament. Journal of Orthopaedic Research 15, 278–284.

Maker, B.N., Ferencz, R.M., Hallquist, J.O., 1990. NIKE3D: a nonlinear, implicit, three-dimensional finite element code for solid and structural mechanics. Lawrence Livermore National Laboratory Technical Report UCRL-MA-105268.

Markolf, K.L., Wascher, D.C., Finerman, G.A., 1993. Direct in vitro measurement of forces in the cruciate ligaments. Part II: the effect of section of the posterolateral structures. Journal of Bone and Joint Surgery 75A, 387–394.

Miyasaka, K.C., Daniel, D.M., Stone, M.L., Hirshman, P., 1991. The incidence of knee ligament injuries in the general population. American Journal of Knee Surgery 4, 3–8.

Ng, G.Y., Oakes, B.W., Deacon, O.W., McLean, I.D., Eyre, D.R., 1996. Long-term study of the biochemistry and biomechanics of anterior cruciate ligament-patellar tendon autografts in goats. Journal of Orthopaedic Research 14, 851–856.

Pfaeffle, J., Weiss, J., Gardiner, J., Fischer, K., Manson, T., et al., 2000. The stress and strain distribution in the interosseous ligament of the human forearm varies with forearm rotation. Transactions of the 46th Meeting of the Orthopaedic Research Society 25, 140.

Puso, M.A., Weiss, J.A., 1998. Finite element implementation of anisotropic quasilinear viscoelasticity. ASME Journal of Biomechanical Engineering 120, 62–70.

Quapp, K.M., Weiss, J.A., 1998. Material characterization of human medial collateral ligament. ASME Journal of Biomechanical Engineering 120, 757–763.

Salehpour, A., Butler, D.L., Proch, F.S., Schwartz, H.E., Feder, S.M., et al., 1995. Dose-dependent response of gamma irradiation on mechanical properties and related biochemical composition of goat bone–patellar tendon–bone allografts. Journal of Orthopaedic Research 13, 898–906.

Simbeya, K.W., Shrive, N.G., Frank, C.B., Matyas, J.R., 1992. A micromechanical finite element model of the rabbit medial collateral ligament. In: Middleton, J., Pande, G., Williams, K. (Eds.), Recent Advances in Computer Methods in Biomechanics and Biomedical Engineering. Gordon and Breach, Swansea, UK, pp. 240–249.

Simo, J.C., Hughes, T.J.R., 1998. Computational Inelasticity. New York.

Thornton, G.M., Leask, G.P., Shrive, N.G., Frank, C.B., 2000. Early medial collateral ligament scars have inferior creep behaviour. Journal of Orthopaedic Research 18, 238–246.

Veronda, D.R., Westmann, R.A., 1970. Mechanical characterization of skin—finite deformations. Journal of Biomechanics 3, 111–124.

Wang, C.J., Walker, P.S., Wolf, B., 1973. The effects of flexion and rotation on the length patterns of the ligaments of the knee. Journal of Biomechanics 6, 587–596.

Warren, L.F., Marshall, J.L., Girgis, F., 1974. The prime static stabilizer of the medial side of the knee. Journal of Bone and Joint Surgery 56-A, 665–674.

Weiss, J.A., Maker, B.N., Govindjee, S., 1996. Finite element implementation of incompressible, transversely isotropic hyperelasticity. Computer Methods in Applied Mechanics and Engineering 135, 107–128.

Weiss, J.A., Schauer, D.A., Gardiner, J.C., 1996. Modeling contact in biological joints using penalty and augmented Lagrangian methods. Proceedings of the ASME Winter Annual Meeting BED-33, 347–348.

Wilson, A.N., Shelton, F., Chaput, C., Frank, C., Butler, D., Shrive, N., 1997. The shear behaviour of the rabbit medial collateral ligament. Medical Engineering and Physics 19, 652–657.

Woo, S.L., Niyibizi, C., Matyas, J., Kavalkovich, K., Weaver-Green, C., Fox, R.J., 1997. Medial collateral knee ligament healing. Combined medial collateral and anterior cruciate ligament injuries studied in rabbits. Acta Orthopaedica Scandinavica 68, 142–148.

Zhu, W., Mow, V.C., Koob, T.J., Eyre, D.R., 1993. Viscoelastic shear properties of articular cartilage and the effects of glycosidase treatments. Journal of Orthopaedic Research 11, 771–781.